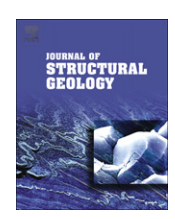
ELSEVIER

Contents lists available at ScienceDirect

## Journal of Structural Geology

journal homepage: www.elsevier.com/locate/jsg



# Compaction control of topography and fault network structure along strike-slip faults in sedimentary basins

Christoph E. Schrank\*,1, Alexander R. Cruden

Department of Geology, University of Toronto, 22 Russell Street, Toronto, ON M5S 3B1, Canada

#### ARTICLE INFO

Article history:
Received 14 May 2009
Received in revised form
4 November 2009
Accepted 5 November 2009
Available online 11 November 2009

Keywords: Analogue modelling Strike-slip faults Topography Compaction Dilatancy Shear box

#### ABSTRACT

Strike-slip faults commonly display structurally complex areas of positive or negative topography. Understanding the development of such areas has important implications for earthquake studies and hydrocarbon exploration. Previous workers identified the key factors controlling the occurrence of both topographic modes and the related structural styles. Kinematic and stress boundary conditions are of first-order relevance. Surface mass transport and material properties affect fault network structure. Experiments demonstrate that dilatancy can generate positive topography even under simple-shear boundary conditions. Here, we use physical models with sand to show that the degree of compaction of the deformed rocks alone can determine the type of topography and related surface fault network structure in simple-shear settings. In our experiments, volume changes of  $\sim 5\%$  are sufficient to generate localized uplift or subsidence. We discuss scalability of model volume changes and fault network structure and show that our model fault zones satisfy geometrical similarity with natural flower structures. Our results imply that compaction may be an important factor in the development of topography and fault network structure along strike-slip faults in sedimentary basins.

© 2009 Elsevier Ltd. All rights reserved.

#### 1. Introduction

Strike-slip faults occur from plate-boundary to local scales and their rich structural inventory is important for the exploration and development of hydrocarbon deposits in sedimentary basins (Harding, 1985; Sylvester, 1988). Strike-slip faults appear as narrow linear features at the surface with lengths up to thousands of kilometres. In detail, they consist of a complex, anastomosing network of smaller faults. Within these networks, areas of either positive or negative topography occur on various scales, e.g., pressure ridges, sag ponds, positive and negative flower structures, pop-ups, and pull-apart basins (Bergerat et al., 2003; Harding, 1985; Mann, 2007; Sylvester, 1988).

Stress- and kinematic-boundary conditions exert the first-order control on the generation of topography and fault network structure (Braun, 1994; Dresen, 1991; Koons and Henderson, 1995; Mann, 2007; Naylor et al., 1986; Richard et al., 1995). A component of fault-normal stress seems required to create topography. However, numerical (Braun, 1994) and physical (Le Guerroué and Cobbold, 2006; Schöpfer and Steyrer, 2001) models show that dilatancy can

induce positive topography in simple-shear settings. Host rock rheology (Dresen, 1991), the thickness of the sheared rock layer (Schöpfer and Steyrer, 2001; Tchalenko, 1970), and syndeformational erosion and sedimentation (Le Guerroué and Cobbold, 2006) affect fault network structure but do not switch the polarity of topography. Here we use analogue experiments with sand to show that the degree of compaction of the deformed rock can determine the topographic mode and invoke characteristic differences in surface fault network structure. This has important implications for strike-slip faults in sedimentary basins.

### 2. Methods

We performed ten experiments with loosely and densely packed sand. Since the results are consistent with respect to fault zone width, number of faults, and topography, only two representative experiments are shown. We use a simple-shear box with side walls and a basal cut as velocity discontinuity (Fig. 1a). One half of the box is driven by a piston at a constant rate of 2.5 cm/h. A 4 cm thick layer of quartz sand with a mean grain size of 200  $\mu$ m is employed as analogue for upper-crustal brittle rocks (Lohrmann et al., 2003). We varied its physical properties by sifting or pouring it into the box (Krantz, 1991). The sifted sand has a density of 1700 kg/m³ and rheology, determined in a Hubbert-type shear apparatus with Plexiglas walls similar to that used by Lohrmann et al. (2003),

<sup>\*</sup> Corresponding author. Tel.: +61 8 6488 2680; fax: +61 8 6488 1037. E-mail address: cschrank@cyllene.uwa.edu.au (C.E. Schrank).

<sup>&</sup>lt;sup>1</sup> Present address: School of Earth and Environment, The University of Western Australia. 35 Stirling Highway. Crawley. WA 6009. Australia.

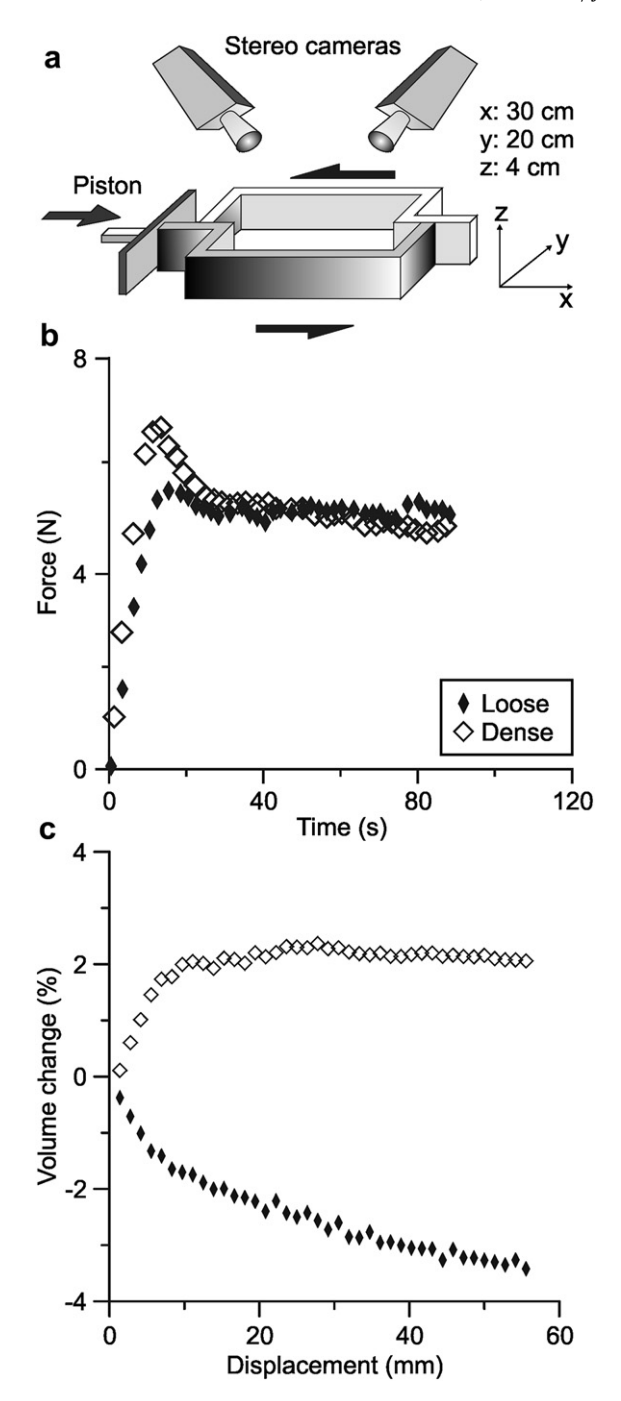


**Fig. 1.** a) Experimental setup. Box dimensions with respect to coordinate system are given in figure. b) Results of a Hubbert-type shear test on a 4 cm layer of loose and dense sand, respectively. c) Plots of total-volume change as a function of piston displacement in models with loose and dense sand.

characterized by transitional strain hardening, followed by strain softening until stable strength is reached (Lohrmann et al., 2003) (Fig. 1b). The peak and stable friction angles are 39° and 27°, respectively. Assuming a quartz grain density of 2660 kg/m³, the sifted sand has a porosity of 36.1%. Pouring results in a higher filling velocity and under-compacted sand with a density of 1474 kg/m³, porosity of 44.6%, and peak and stable friction angles 30° and 27°, respectively. Cohesion at peak strength is 60 and 80 Pa for sifted and poured sand, respectively, with an uncertainty of ~30% inherent to the measurement method (Lohrmann et al., 2003).

Since the basal normal stresses in our experiments exceed 570 Pa, the critical stress is friction-controlled.

We note that the above mechanical data do not account for sidewall friction of the shear apparatus. Mourgues and Cobbold (2003) point out that a silo effect can lead to an overestimation of normal stress in shear tests and therefore erroneous friction coefficient and cohesion values. If we apply the correction given by Mourgues and Cobbold (2003) assuming a friction coefficient,  $\mu_s$ , of 0.35 between the shear box walls (Plexiglass) and our sand and a ratio of horizontal to vertical stress, K, of 0.5, we obtain peak and stable friction angles of  $\sim 50^{\circ}$  and  $\sim 36^{\circ}$ , respectively, for sifted sand, and  $\sim 40^{\circ}$  and  $\sim 36^{\circ}$ for poured sand. The cohesion values decrease to 20 Pa and 37 Pa for sifted and poured sand, respectively. This correction is sensitive to the choice of  $\mu_s$  and K, which are assumed here to be similar to those of the experiments of Mourgues and Cobbold (2003). However, in this paper, we focus on the effect of differences in initial porosity of sand (i.e., its degree of compaction) on strike-slip experiments. The given mechanical data (friction-corrected and -uncorrected) bracket the true properties of our sand, and a more precise mechanical characterization is beyond the scope of this work.

We monitored the experiments with a stereoscopic 3D Particle Imaging Velocimetry (PIV) system (manufactured by LaVision GmbH, Germany). Images were recorded every 100 s with two monochrome CCD cameras from above (Fig. 1a) providing 3D measurements of the model surfaces with an accuracy of 0.1 mm. The resulting digital elevation models were used to compute volume changes by subtracting the initial undeformed model surface from deformed model surfaces over time. Camera resolution was  $\sim 90$  pixel/cm. 3D surface velocity fields are derived by cross-correlation of sequential images (Adam et al., 2005). We determined 3D surface displacement vectors in a  $\sim 16 \times 14$  cm² area in the box centre with an accuracy of < 0.1 mm for 2  $\times$  2 mm² search windows. Strains were calculated from the displacement gradients.

#### 3. Results

The differences in topographic evolution for loose and dense sand are striking. In loose sand, the whole surface begins to subside towards the piston at the onset of deformation (Fig. 2). The asymmetry of the subsidence is attributed to vibrations transmitted from the stepper motor close to the piston. A channel-like basin propagates along the fault system towards the rear end of the model (Figs. 2 and 3). A rhomb-shaped basin, similar to a pull-apart basin, opens in the model centre (Fig. 2b,c). Maximum elevation difference is ~5 mm. The total volume decreases by 3.4% (Fig. 1c), the volume within the fault zone alone decreases by 4.2%. In contrast, positive topography develops in dense sand. It is focused in a fault-bound wedge in the model centre (Figs. 2 and 3). Topographic growth becomes increasingly localized, the maximum elevation difference is 7 mm and the maximum total volume increase is 2.4% (Fig. 1c). Volume increase in the wedge alone amounts to 5.1%.

The surface fault network geometry differs accordingly, as illustrated by maps of incremental horizontal shear strain  $Exy = \mathrm{d}D_x/\mathrm{d}y$ , where  $D_x$  is displacement in x-direction, and transversal shear strain profiles through the model centre (Fig. 3). The strain increments correspond to 0.7 mm displacement steps. Loose sand displays a narrow fault network consisting of synthetic Riedel shears linked by P and Y shears (Tchalenko, 1970). Dense sand develops a broader fault network comprising three main faults in synthetic Riedel orientation. The outer faults bound the wedge while the middle fault is in its centre. Initially, the middle fault consists of linked synthetic Riedel shears that are visible but below PIV resolution. At later stages the entire fault network is dominated by large Riedel shears that are less strongly linked at the surface and longer than those in loose sand.

## Download English Version:

# https://daneshyari.com/en/article/4733692

Download Persian Version:

https://daneshyari.com/article/4733692

Daneshyari.com